

Acoustic transparency and slow sound using detuned acoustic resonators

Arturo Santillán* and Sergey I. Bozhevolnyi

Institute of Technology and Innovation, University of Southern Denmark, Niels Bohrs Allé 1, 5230 Odense M, Denmark

(Received 25 July 2011; published 30 August 2011)

We demonstrate that the phenomenon of acoustic transparency and slow sound propagation can be realized with detuned acoustic resonators (DAR), mimicking thereby the effect of electromagnetically induced transparency (EIT) in atomic physics. Sound propagation in a pipe with a series of side-attached DAR, with adjacent DAR units spaced by a distance much smaller than the wavelength, is analyzed. We show that such a chain of DAR units forms an analog of one-dimensional (1D) metamaterial with unique properties of dispersion and transmission, revealing the possibility of slowing sound (at 2 kHz) down by ~ 100 times within the 40-Hz-broad transparency window. Preliminary experiments with two resonators detuned from the central frequency of 1.2 kHz verify the occurrence of the transparency effect.

DOI: [10.1103/PhysRevB.84.064304](https://doi.org/10.1103/PhysRevB.84.064304)

PACS number(s): 43.35.+d, 42.50.Gy, 43.20.+g

I. INTRODUCTION

The phenomenon of electromagnetically induced transparency (EIT) involves the laser-induced coherence of atomic states leading to quantum interference between the excitation pathways controlling the optical response, which is thereby modified exhibiting the enhanced transmission along with strong dispersion and slowdown of light propagation.¹ Realization of EIT-like response with classical oscillator systems has been reported for a large number of photonic and plasmonic configurations (see recent reviews^{2,3}). Considerably less attention has been paid to the implementation of EIT-like phenomena in acoustics, where the main emphasis was insofar on theoretical considerations being devoted to coupled resonators,⁴ sonic crystals,⁵ and differently oriented rods.⁶ While in the first configuration⁴ the transparency is achieved due to distant coupling of two resonators grafted along a tube (similarly to the coupled resonator-induced transparency known in photonics⁷), the EIT-like transparency in the latter⁶ occurs due to coupling between the rod-resonator modes with highly different quality factors Q in a complete analogy with the plasmon-induced transparency by near-field coupled radiative and subradiant (dark) plasmonic elements.⁸

The EIT phenomenon can be considered using two alternative ways: as resulting from the destructive interference between two pathways involving either the *bare*, dipole-allowed, and metastable states or, *equivalently*, the doublet of *dressed* states (e.g., created by strong pump radiation) representing two closely spaced resonances decaying to the same continuum.¹ While these two physical pictures are equivalent when dealing with EIT in atomic systems, their classical realization with (photonic or acoustic) systems, whose responses are determined by their configurations and *not* electromagnetically induced as in EIT, *depends* on the EIT mechanism that is imitated. The first picture suggests employing strongly coupled oscillators resonating at the same frequency but having very different (low and high) Q -factors.^{6,8} Alternatively viewed, EIT is achieved due to the cancelation of opposite contributions from two resonances, which are equally spaced but with opposite signs of detuning from the probe frequency, due to the Fano-like interference of the decay channels.^{1-3,9} For classical realization of this dressed-state picture of EIT, one can employ detuned (but otherwise identical) resonators that

are, for example, side-coupled at the *same* place to a bus waveguide.¹⁰

In this paper we demonstrate the use of detuned acoustic resonators (DAR) side-attached to an acoustic pipe for the realization of acoustic transparency in a narrow frequency range accompanied with significant slowdown of sound propagation, thus emulating the dressed-state picture of EIT. Contrary to the previously considered configuration of two side resonators grafted at two sites on a tube,⁴ where the transparency effect is produced with the two resonators separated by a distance of about one wavelength, two DAR are located at the *same* axial position in our system constituting a unit referred hereafter as a cell. Importantly, the spatial extension of such a cell in the direction of propagation can be deeply subwavelength, implying that DAR unit cells can be *subwavelength*-spaced along a pipe. We demonstrate that subwavelength-spaced DAR cells form thereby a one-dimensional (1D) *acoustic metamaterial* with unique dispersion and filtering properties. This configuration opens yet another research avenue in a rapidly expanding field of acoustics metamaterials that comprises metamaterials with negative bulk modulus and mass density,¹¹⁻¹³ including those utilizing arrays of subwavelength Helmholtz resonators,¹⁴⁻¹⁶ and negative refractive index,¹⁷ as well as metamaterials developed for subwavelength focusing,^{18,19} and acoustic transparency.²⁰

II. THEORY

The acoustic metamaterial configuration studied in this work is formed by an acoustic waveguide of constant cross-sectional area S with a series of attached pairs of (detuned) Helmholtz resonators (Fig. 1). The waveguide, extended along the x -axis, has cross-sectional dimensions much smaller than the shortest wavelength in the considered frequency band, allowing thus only plane waves to propagate. Paired resonators are placed at the same axial position forming a unit cell. The resonance frequency of one resonator in the cell is slightly different from the other one. The constant distance l_c between the centers of the openings of two adjacent resonators is considered as the length of the cell and assumed to be much smaller than the sound wavelength. We note in passing that sound transmission in a waveguide with a series of side-attached Helmholtz resonators separated by

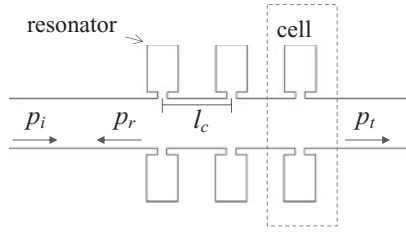


FIG. 1. Diagram of the waveguide with a series of Helmholtz resonators. Two resonators at the same axial position are referred as one cell; the constant distance l_c between adjacent resonators is the length of the cell.

subwavelength distances has been studied for configurations, in which resonance frequencies of the resonators increased progressively along the waveguide in order to obtain a broader frequency stopband as compared to that of an individual resonator.²¹

In the following analysis we consider the waveguide to be infinite in length with a monochromatic incident sound wave $p_i = A_i \exp(-jkx)$ at the angular frequency ω approaching the series of cells from the left (here k is the wave number and A_i is the complex amplitude). Let A_r and A_t denote, respectively, the complex amplitudes of the wave reflected from the start of the first cell and the wave transmitted at the end of the cell array. All the resonators are assumed to have identical openings and necks. The acoustic impedance (the ratio between the sound pressure and volume velocity) just outside the opening of the first resonator in a cell is given by $Z_1 = R_a + j(\omega M - K_1/\omega)$, where R_a , M , K_1 are, respectively, the acoustic resistance, inertance, and stiffness of the first resonator. In addition, $M = \rho L_{ef}/S_{res}$ and $K_1 = \rho c^2/V_1$, where ρ is the medium density, c is the sound speed, V_1 is the volume of the resonator, S_{res} is the cross-sectional area of the neck, and L_{ef} its effective length. Accordingly, a similar expression describes the acoustic impedance Z_2 at the opening of the second resonator in the cell.

We first consider only one cell in the waveguide, so that the ratio A_t/A_i is given by the following simple expression²²:

$$\frac{A_t}{A_i} = \frac{2Z_c}{Z + 2Z_c}, \tag{1}$$

where $Z = \rho c/S$, and $Z_c = Z_1 Z_2 / (Z_1 + Z_2)$ is the combined acoustic impedance of the two resonators. The transmission spectrum $|A_t/A_i|^2$ for the one-cell system, in which the individual resonances were designed to be $f_1 = 1872$ Hz and $f_2 = 2135$ Hz, features a narrow EIT-like transparency peak at the central frequency of 2000 Hz [Fig. 2(a)] that manifests the phenomenon of acoustic transparency due to coherent (destructive) interference of responses from individual resonators, which otherwise exhibit quite low (individual) transmission at this frequency. The chosen parameter are $\rho = 1.2$ kg/m³, $c = 342$ m/s, $S = 3.14$ cm², $S_{res} = 0.64$ cm², $L_{ef} = 7.2$ mm, $V_1 = 7.47$ cm³, $V_2 = 5.74$ cm³, and $R_a = 2000$ Pa·m/s. The value of R_a , which accounts for energy losses due to viscosity and thermal conduction in the resonators, was chosen (from a realistic range) to illustrate the influence of loss in the system that would still result in a relatively high transmission in the acoustic transparency window. Similarly to the EIT phenomenon in quantum optics¹ and photonics,^{2,3} the phase of transmitted wave varies drastically across the transmission window, exhibiting the phase change of $\sim 170^\circ$ in the frequency range of ~ 260 Hz [Fig. 2(b)] and reaching the maximum slope of $\sim 2.3^\circ/\text{Hz}$ at the frequency of ~ 2 kHz. Such a strong phase variation implies the possibility of a significant reduction in the sound group velocity similar to the effect of slowing down the propagation of optical pulses¹⁻³ when using a series of DAR unit cells.

For a periodic array of N cells separated by the distance l_c (Fig. 1), the waveguide segment that includes Helmholtz resonators can be regarded as an acoustical two-port system.²³ In this way the sound pressure amplitude p_{in} at $x = 0$ (the assumed position of the first cell) and the volume velocity U_{in} at the same location can be related to the transmitted sound pressure and the corresponding volume velocity as

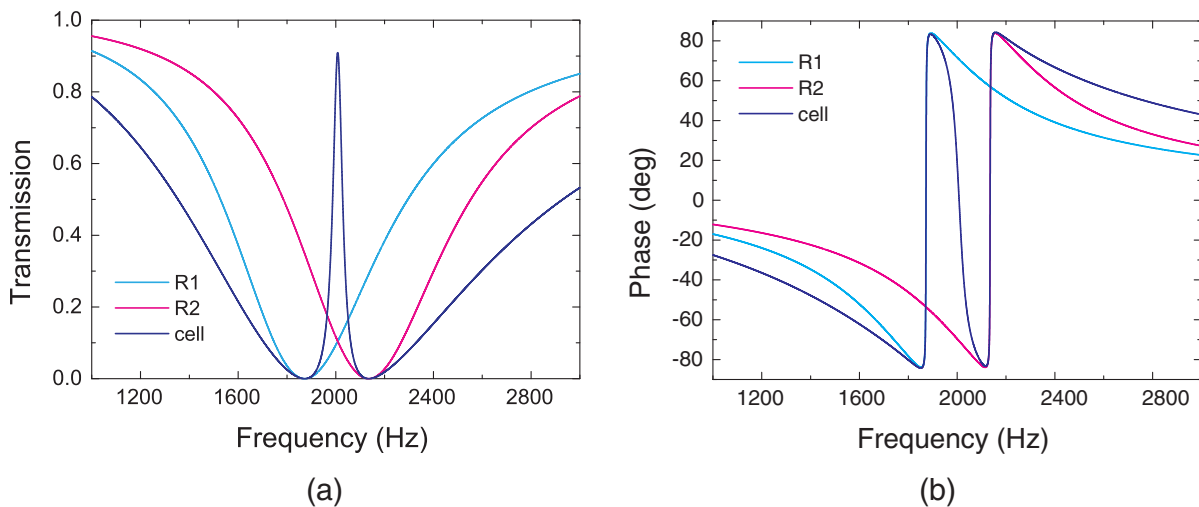


FIG. 2. (Color online) (a) Transmission vs frequency for one cell coupled to the waveguide, where the induced transparency effect is produced in the vicinity of 2 kHz. The curves for each of the two resonators, R1 and R2, are also included. (b) The phases of the transmitted waves corresponding to each of the three cases.

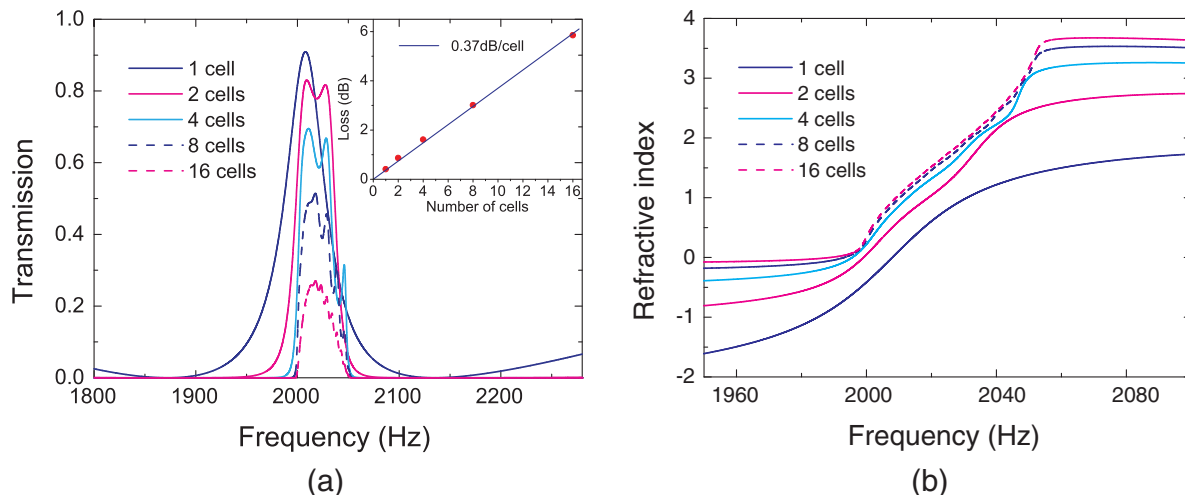


FIG. 3. (Color online) The left graph presents several curves of transmission vs frequency for waveguides with different numbers of cells. The right graph shows that the corresponding curves of the refractive index in the frequency band of induced transparency approach a limit value. In this case the group refractive index is approximately 100 for the studied acoustic system. The inset in the left graph depicts a linear relation between the logarithm of losses at the peak transmission in the transparency region vs the number of cells.

$[p_{\text{in}} \ U_{\text{in}}]^T = \mathbf{M}[A_t \ A_t/Z]^T$, where matrix \mathbf{M} is given by $\mathbf{M} = (\mathbf{M}_C \ \mathbf{M}_T)^{N-1} \mathbf{M}_C$ and

$$\mathbf{M}_C = \begin{bmatrix} 1 & 0 \\ 1/Z_C & 1 \end{bmatrix}, \quad \mathbf{M}_T = \begin{bmatrix} \cos(kl_c) & iZ \sin(kl_c) \\ i \sin(kl_c)/Z & \cos(kl_c) \end{bmatrix} \quad (2)$$

The pressure amplitude reflection coefficient can then be calculated²³ as $R = A_r/A_i = (Z_{\text{in}} - Z)/(Z_{\text{in}} + Z)$, where $Z_{\text{in}} = p_{\text{in}}/U_{\text{in}}$. Consequently, complex amplitudes of the incident and transmitted waves are connected with the relation $[A_t \ A_t/Z]^T = \mathbf{M}^{-1}[(1 + R)A_i \ (1 - R)A_i/Z]^T$, from which transmission can be obtained. Note that this method of obtaining the transmission in the system is equivalent to the previously used method,⁴ which is based on the interface response theory of continuous media.

Considering a series of DAR cells in which the physical and geometrical parameters are the same as in the example for one cell discussed previously, we observed that the transmission peak decreases with a number of cells due to energy losses introduced by the acoustic resistance R_a [Fig. 3(a)]. We would like to stress that the cell length $l_c = 2.1$ cm corresponding to $1/8$ of the sound wavelength at the frequency of 2 kHz was chosen to be significantly below the wavelength in order to avoid inter-cell interference and, thereby, realize an analog of 1D-acoustic metamaterial. We have indeed found a linear relation between the insertion loss (at the transparency frequency) expressed in dB and the number of cells [see inset in Fig. 3(a)], which is expected for a metamaterial supporting a single propagating mode.⁸ The propagation loss of ~ 0.37 dB/cell, which can be adjusted by controlling the acoustic resistance, allows one to use such a series of several cells in practice, e.g., for designing narrow-band transmission filters. It should be noted that the width and depth of the absorption band (on both sides of the transparency window) increases considerably with the number of cells [Fig. 3(a)].

Regarding a series of DAR cells as a 1D metamaterial, one can determine the corresponding effective refractive index $n(f)$ using the following relation:

$$n(f) = -\frac{\varphi(f)}{\omega N l_c / c}, \quad (3)$$

where φ is the phase (in radians) of the transmitted wave. The refractive index calculated for the considered system using Eq. (3) indeed exhibited the dispersion that converges with the increase in the number of cells, especially in the transparency window centered at ~ 2020 Hz [Fig. 3(b)]. In the region of normal dispersion, i.e., when $dn/df > 0$, one can determine the group refractive index $n_{\text{gr}}(f)$ as follows:

$$n_{\text{gr}}(f) = n(f) + f \frac{dn(f)}{df}. \quad (4)$$

It is seen that, for two or more cells in the waveguide, the slopes of the dispersion curves and, thereby, the corresponding group refractive indexes are practically the same in the transparency window [Fig. 3(b)], reaching the value of ~ 100 as estimated from Eq. (4). Our simulations showed that even larger group indexes can be realized by decreasing the cell length and/or detuning frequency. It should however be born in mind, when adjusting the detuning, that a trade-off exists between the transmission level and the dispersion slope within the transparency window.

III. EXPERIMENTAL RESULTS

To experimentally demonstrate the suggested approach for acoustic transparency, a system with one cell was implemented using an acrylic tube with inner diameter of 2 cm and length of 4 m as a waveguide (Fig. 4). The Helmholtz resonators were 14-mm-diameter cylinders (of different length) made of plastic and having necks with a circular diameter of 4.4 mm. This small neck size was chosen to achieve a better correspondence to the assumptions in the theoretical model based on lumped parameters. In this way a good agreement between the above

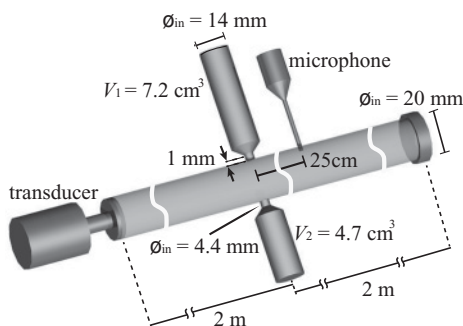


FIG. 4. Diagram of the experimental set up.

theoretical description and experimental results was expected, albeit at the expense of introducing large energy losses when using necks with a small diameter. For each resonator, the shape of the surface around its mouth matched the inner curved wall of the tube waveguide. The measured volumes of the resonators were 7.2 and 4.7 cm³, ensuring thereby the detuning in their resonance frequencies. The effective length of the neck of resonators was measured to be 5.4 mm. For this purpose only one resonator was attached to the waveguide, and the resonance frequency was measured for different volumes of its cavity.

A magnetostrictive transducer with a short impulse response was used to generate the sound wave. A rectangular impulse with a width of 200 μs was fed to the transducer, which produced a response of less than 2 ms. The transducer was coupled to one end of the tube, and the resonators were placed 2 m from the source (Fig. 4). A probe microphone measured the sound field in the pipe at the distance of 25 cm after the location of the resonators. The inner and outer diameters of the probe were 1.3 and 2 mm, respectively, so that its influence on the conducted measurements could be neglected. During the data acquisition, the measured signal was cut after 11 ms from the instant at which the sound wave was detected by the microphone. In this way the reflections of sound from the ends of the pipe were excluded from the consideration.

To obtain the pressure transmission coefficient A_t/A_i as a function of frequency, first the transfer function H_0 between the signal picked up by the microphone and the input signal to the transducer was determined in the waveguide without the resonators. This transfer function represents the frequency response of the system, i.e., that of the acoustic source and detector as well as the transmission spectrum of the sound wave propagating along the tube from the sound source to the microphone position. In the second part of the experiment the transfer function H_1 between the sound pressure measured by the microphone with one or two resonators coupled to the tube and the input signal to the transducer was obtained. Thus the pressure transmission coefficient was given by $A_t/A_i = H_1/H_0$. The average value of 100 measurements was taken to determine H_1/H_0 in order to minimize random errors.

A very good agreement between theoretical results and experimental data was obtained for the amplitude and phase transmission spectra measured with the individual resonators and their combination (Fig. 5). The value of the acoustic resistance, $R_a = 99480 \text{ Pa}\cdot\text{m/s}$ used in the theoretical model was determined by fitting in order to adjust the calculated peak of transmission to the experimental value. The transparency effect was observed in the vicinity of 1200 Hz, where the slope of the phase was $\sim 0.6^\circ/\text{Hz}$. The latter implies [Eq. (4)] that a series of these DAR with the cell length of $\sim 2 \text{ cm}$, which corresponds to 1/14 of the wavelength at 1200 Hz and is still larger than the resonator tube diameter, should result in the group refractive index of ~ 30 . This slowdown factor is favorable compared with the results of previously reported experiments,²⁴ in which the group velocity was slowed to 0.24 of the value of the speed of sound in air by introducing a defect in a periodic 1D-acoustic band-gap array along a waveguide.

IV. CONCLUSION

In summary we have demonstrated that the phenomenon of acoustic transparency and slow sound propagation can be realized with DAR that are placed on both sides of an acoustic pipe with *subwavelength* separation between adjacent DAR cells, forming thereby an analog of 1D-acoustic

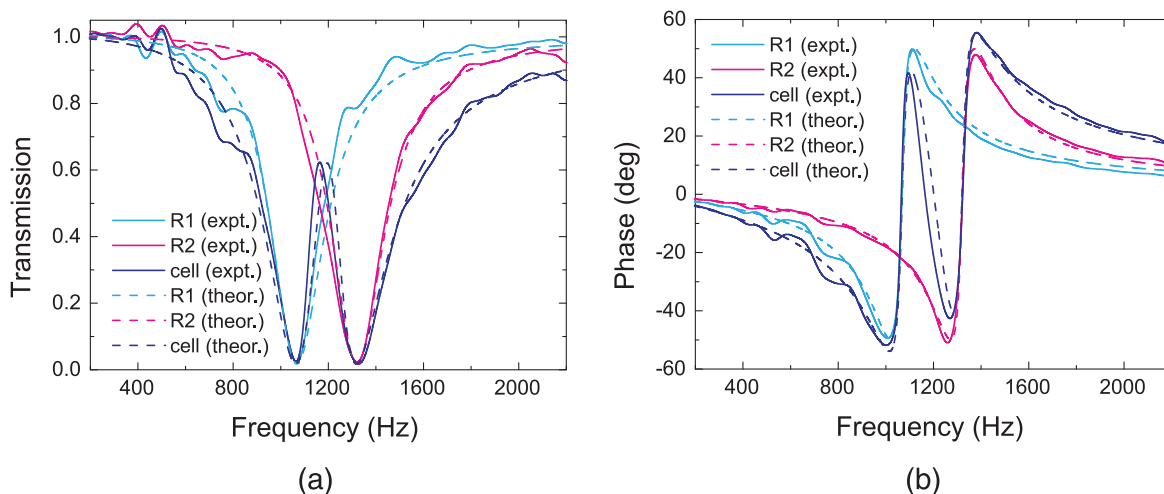


FIG. 5. (Color online) Experimental data and their comparison with theoretical results for transmission of sound in a waveguide with one cell. The curves corresponding to the individual resonators are also shown.

metamaterial with *unique* dispersion and filtering properties. Analyzing sound propagation in an acoustic pipe with a series of side-attached subwavelength-spaced DAR, we have shown the possibility of slowing sound (at 2 kHz) down by ~ 100 times within the 40-Hz-broad transparency window for realistic DAR parameters. Preliminary experiments with two Helmholtz resonators detuned from the central frequency of 1.2 kHz have confirmed the occurrence of the expected transparency effect featuring the phase slope of $\sim 0.6^\circ/\text{Hz}$

upon transmission. These results with the implemented system represent a step towards the experimental demonstration of the transparency effect in an acoustic metamaterial with several cells. We believe that the suggested approach opens a new and very promising research avenue in the field of acoustic transport as well as acoustic metamaterials, offering new approaches to slowing down the propagation of sound waves and designing narrow-band acoustic transmission filters that can even be subwavelength-sized in the propagation direction.

*Corresponding author: aos@iti.sdu.dk

- ¹K. J. Boller, A. Imamoglu, and S. E. Harris, *Phys. Rev. Lett.* **66**, 2593 (1991).
- ²A. E. Miroshnichenko, S. Flach, and Y. S. Kivshar, *Rev. Mod. Phys.* **82**, 2257 (2010).
- ³B. Luk'yanchuk, N. I. Zheludev, S. A. Maier, N. J. Halas, P. Nordlander, H. Giessen, and C. T. Chong, *Nature Mater.* **9**, 707 (2010).
- ⁴E. H. El Boudouti, T. Mrabti1, H. Al-Wahsh, B. Djafari-Rouhani, A. Akjouj, and L. Dobrzynski, *J. Phys.: Condens. Matter* **20**, 255212 (2008).
- ⁵J. Sánchez-Dehesa, D. Torrent, and L. W. Cai, *New J. Phys.* **11**, 013039 (2009).
- ⁶F. Liu, M. Ke, A. Zhang, W. Wen, J. Shi, Z. Liu, and P. Sheng, *Phys. Rev. E* **82**, 026601 (2010).
- ⁷Q. Xu, S. Sandhu, M. L. Povinelli, J. Shakya, S. Fan, and M. Lipson, *Phys. Rev. Lett.* **96**, 123901 (2006).
- ⁸S. Zhang, D. A. Genov, Y. Wang, M. Liu, and X. Zhang, *Phys. Rev. Lett.* **101**, 047401 (2008).
- ⁹S. I. Bozhevolnyi, A. B. Evlyukhin, A. Pors, M. G. Nielsen, M. Willatzen, and O. Albrektsen, *New J. Phys.* **13**, 023034 (2011).
- ¹⁰Z. Han and S. I. Bozhevolnyi, *Opt. Express* **19**, 3251 (2011).
- ¹¹J. Li and C. T. Chan, *Phys. Rev. E* **70**, 055602 (2004).
- ¹²Y. Ding, Z. Liu, C. Qiu, and J. Shi, *Phys. Rev. Lett.* **99**, 093904 (2007).
- ¹³L. Fok and X. Zhang, *Phys. Rev. B* **83**, 214304 (2011).
- ¹⁴N. Fang, D. Xi, J. Xu, M. Ambati, W. Srituravanich, C. Sun, and X. Zhang, *Nature Mater.* **5**, 452 (2006).
- ¹⁵Z. G. Wang, S. H. Lee, C. K. Kim, C. M. Park, K. Nahm, and S. A. Nikitov, *J. Phys.: Condens. Matter* **20**, 055209 (2008).
- ¹⁶Y. Cheng, J. Y. Xu, and X. J. Liu, *Appl. Phys. Lett.* **92**, 051913 (2008).
- ¹⁷F. Bongard, H. Lissek, and J. R. Mosig, *Phys. Rev. B* **82**, 094306 (2010).
- ¹⁸M. Ambati, N. Fang, C. Sun, and X. Zhang, *Phys. Rev. B* **75**, 195447 (2007).
- ¹⁹S. Guenneau, A. Movchan, G. Pétursson, and S. A. Ramakrishna, *New J. Phys.* **9**, 399 (2007).
- ²⁰X. Zhou and G. Hu, *Phys. Rev. E* **75**, 046606 (2007).
- ²¹J. Fey and W. M. Robertson, *J. Appl. Phys.* **109**, 114903 (2011).
- ²²L. E. Kinsler, A. R. Frey, A. B. Coppens, and J. V. Sanders, *Fundamentals of Acoustics*, (John Wiley & Sons, New York, 2000), p. 291.
- ²³A. D. Pierce, *Acoustics: An Introduction to Its Physical Principles and Applications*, (McGraw-Hill, New York, 1981), pp. 350–354.
- ²⁴W. M. Robertson, C. Baker, and C. B. Bennett, *Am. J. Phys.* **72**, 255 (2004).